Chi *et al. Nanoscale Research Letters* (2020) 15:79
https://doi.org/10.1186/s11671-020-03307-y

Nanoscale Research Letters

NANO EXPRESS Open Access

Thermoelectric Effect in a Correlated Quantum Dot Side-Coupled to Majorana Bound States

Feng Chi[1], Zhen-Guo Fu[2*], Jia Liu[3], Ke-Man Li[3], Zhigang Wang[2] and Ping Zhang[2]

Abstract

We theoretically study the thermoelectric effect in a hybrid device composed by a topological semiconducting nanowire hosting Majorana bound states (MBSs) and a quantum dot (QD) connected to the left and right non-magnetic electrodes held at different temperatures. The electron-electron Coulomb interactions in the QD are taken into account by the non-equilibrium Green's function technique. We find that the sign change of the thermopower, which is useful for detecting the MBSs, will occur by changing the QD-MBS hybridization strength, the direct overlap between the MBSs at the opposite ends of the nanowire, and the system temperature. Large value of 100% spin-polarized or pure spin thermopower emerges even in the absence of Zeeman splitting in the QD or magnetic electrodes because the MBSs are coupled to electrons of only one certain spin direction in the QD due to the chiral nature of the Majorana fermions. Moreover, the magnitude of the thermopower will be obviously enhanced by the existence of MBSs.

Keywords: Thermoelectric effect, Quantum dot, Majorana bound states, Thermopower

Introduction

The preparation and detection of zero-energy Majorana bound states (MBSs) are of particular importance in modern condensed matter physics. Fundamentally, the MBSs are solid state counterpart of Majorana fermions and are associated with non-Abelian statistics that can enable topologically protected quantum information with potential applications in quantum computation free from decoherence [1–3]. Apart from this, the MBSs are also promising in design of high-efficiency electronic devices, such as the spintronics [4]. Well-separated MBSs can be prepared in various systems, of which the most important schemes include non-centrosymmetric superconductors [5], three- or two-dimensional topological insulators coupled to superconductors [6], electrostatic defects in topological superconductors [7], p-wave superconductors [8], the semiconducting [9] or ferromagnetic [10] nanowires with native strong spin-orbit interaction proximitization to a conventional s-wave superconductors, and Josephson junctions [11].

As for the detection of MBSs, it is also quite challenging because the Majorana fermions are their own antiparticles and charge-neutral due to their intrinsic particle-hole symmetry. A variety of experiments have been carried out to verify the existence of MBSs through phenomena such as the 4π periodic Josephson current phase in junctions between topological superconductors [12], half-integer conductance plateau at the coercive field in a hybrid structure composing of topological superconductors and topological quantum anomalous Hall insulator [13], tunneling spectroscopy using Rashba nanowires coupled to the bulk s-wave superconductors [14], and zero bias of the differential conductance at the edges of the wires [14, 15]. However, these phenomena have other possible physical origins except for MBSs, and alternative schemes then have been proposed. One of them is

*Correspondence: fu_zhenguo@iapcm.ac.cn
[2]Institute of Applied Physics and Computational Mathematics, No. 6 Huayuan Road, Haidian District, Beijing, 100088, China
Full list of author information is available at the end of the article

the hybridization of MBSs with other nanoscale structures, such as the zero-dimensional quantum dot (QD) in which the energy levels, electron-electron Coulomb interactions, particle numbers, and coupling strength to external environment are all well controllable [16, 17]. At low temperature, a half-maximum conductance when the energy level of the QD is aligned to the Fermi energy in the leads was theoretically predicted as a clear evidence of the formation of a pair of MBSs [18]. This result is completed unchanged by the adjusting of the QD energy level [19] and has successfully been observed in experiment in a QD coupled to an InAs-Al nanowire [20]. Recently, optical schemes based on QD structure were also theoretically proposed to detect the MBSs with the help of optical pump-probe technique. [21, 22] In ring- or T-shaped QD-based systems, the quantum interference phenomena are drastically affected by the MBSs [23–25] and then can be used for the detection scheme with the help of, for example, the Fano effect [26–28].

Recently, there are also some work concerning detection of the MBSs via thermoelectric effect, which focuses on the conversion between electrical and thermal energies. This old research topic gains renewed attention due to the rapid progress of growth and fabrication of mesoscopic devices and nanostructures, in which the thermoelectric performances are obviously improved [29, 30]. High-efficiency energy harvesters based on QDs that are defined on such as a GaAs/AlGaAs interface two-dimensional electron gas have recently been reported [31, 32]. Enhancement of the thermoelectric effect in them can be attributed to the considerable reduction of the thermal conductivity by boundary scattering and the optimization of the electrical transport properties unique in these low-dimensional systems [30–32]. The thermopower (Seebeck coefficient) is the central quantity in thermoelectric effect. It is the strength of a open-circuit voltage in response of a temperature gradient applied in a solid material with free electronic carriers. Hou et al. theoretically predicted that the thermopower between a QD and superconductor hosting a Majorana edge state satisfies the Mott formula and generically does not vanish by using the Landauer-Büttiker formalism [33]. Based on such a property, one can infer the temperature of the Majorana edge state by measuring the differential conductance and the thermopower. Leijnse demonstrated theoretically that the coupling between a QD with tunable energy level and MBSs breaks particle-hole symmetry, and the changes of thermopower provide a new way of proving the existence of Majorana states [34]. The thermoelectric properties in such a setup can also be used to detect the temperature of the superconductor and to extract information about the dissipative decay of MBSs [34]. In a structure with a QD coupled to two electrodes, López et al. showed that the thermopower will change its sign by changing the direct hybridization between the MBSs, a good evidence of the existence of MBSs [35]. The sign change of the thermopower was also subsequently found in systems of a QD with two [36] or three [37] electrodes. Moreover, it was demonstrated that the relationship between the shot noise and thermoelectric quantities may provide a purely electrical way to detect the charge-neutral MBSs [38, 39].

In the present paper, we propose a hybridized system composing of MBSs and a QD coupled to electrodes (see Fig. 1) to study the properties of the thermopower. In the nanosystem we considered, the strong Coulomb interaction in the dot, which has been neglected in previous works [18, 22–24, 34–39], is taken into account. Furthermore, we consider that only one spin component of the QD spin is coupled to the MBSs due to the chiral nature of the MBSs [40]. We find that the sign of the thermopower can be effectively reversed by changing the dot-MBSs coupling strength, the direct hybridization between the MBSs, and the system temperature. The resulted large 100% spin-polarized and pure spin thermopower, which are the corresponding 100% spin-polarized and pure spin currents in closed circuit, are useful in spintronics. The coupling of both the two MBSs to the QD will further enhance the magnitude of the thermopower, but does not change the essential results when only one of the MBSs is coupled to the dot. Based on the presently advanced quantum transport measurements for the MBSs through QD coupled with topological superconducting nanowires, we believe our proposal could be experimentally tested in the future. Additionally, our proposal and findings in this work may provide an excellent way to detecting the formation of the MBSs in QD.

Model and Methods

The effective Hamiltonian of the QD coupled to MBSs and the left and right normal metal electrodes takes the following form [34, 35]:

$$H = \sum_{k\beta\sigma} \varepsilon_{k\beta} c^{\dagger}_{k\beta\sigma} c_{k\beta\sigma} + \sum_{\sigma} \varepsilon_d d^{\dagger}_{\sigma} d_{\sigma} + U d^{\dagger}_{\uparrow} d_{\uparrow} d^{\dagger}_{\downarrow} d_{\downarrow} + \sum_{k\beta\sigma} (V_{k\beta} c^{\dagger}_{k\beta\sigma} d_{\sigma} + H.c) + H_{\mathrm{MBSs}}, \quad (1)$$

where $c^{\dagger}_{k\beta\sigma}$ ($c_{k\beta\sigma}$) creates (annihilates) an electron of momentum k, energy $\varepsilon_{k\beta}$ (its dependence on spin is neglected for normal metal electrode), and spin $\sigma = \uparrow, \downarrow$ in electrode $\beta = L, R$. For the QD, $d^{\dagger}_{\sigma}$ (d_{σ}) is the creation (annihilation) operator of an electron with gate voltage tunable energy level ε_d, spin-σ, and intradot Coulomb interaction U. The coupling strength between the QD and the leads is described by $V_{k\beta}$. The last term H_{MBSs} in Eq. (1) stands for the zero-energy MBSs located on opposite ends of the semiconducting nanowire and their coupling to the QD [18]:

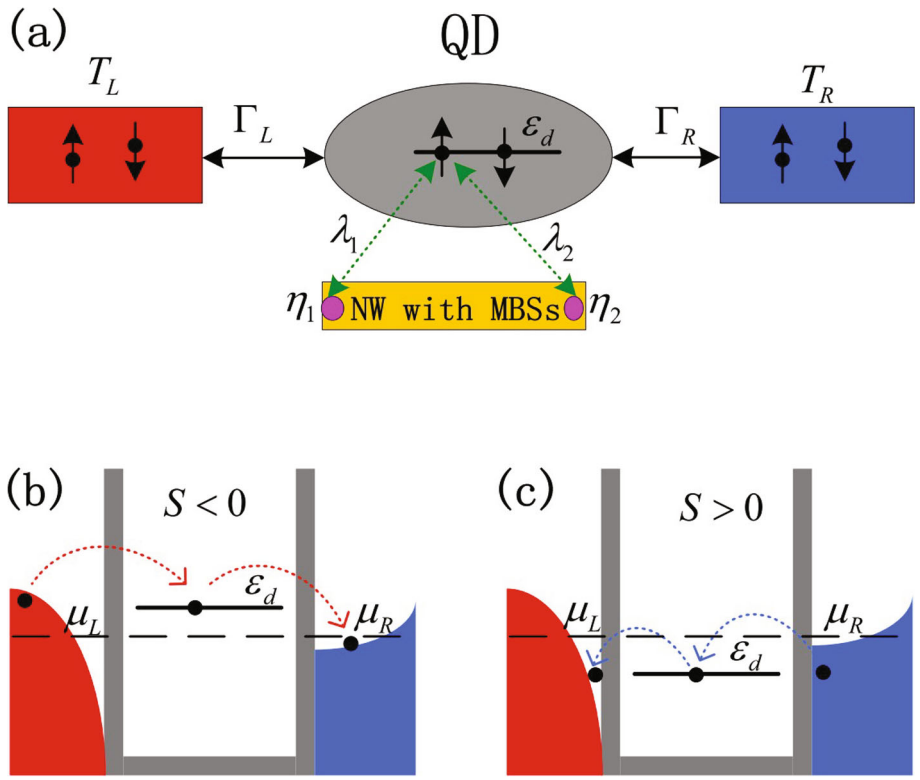

Fig. 1 Schematic of the model (color online). **a** Schematic of the simulation structure composed by a QD with gate-tunable energy level ε_d which can be occupied by either a spin-up or a spin-down electron. The QD is connected to the left and right leads held at different temperatures with coupling strength $\Gamma_{L/R}$. The MBSs $\eta_{1/2}$ are formed in the ends of the semiconducting nanowire and are coupled to the spin-up electrons in the QD due to the chiral nature of the Majorana fermions with strengths of λ_1 and λ_2, respectively. The energy state of spin-up electrons will be changed by MBSs-QD coupling, and then, the strength and sign of the thermopower S will be influenced. In the present model, we assume the temperature of the left lead T_L is higher than that of the right one T_R, and then, there are more electrons (empty states) being excited above (below) the chemical potential in the left lead than those in the right lead. **b**, **c** The electron tunneling processes and the resulted thermopower in the absence of MBSs-QD coupling. In **b**, the QD energy level ε_d is above the chemical potential of the leads $\mu_{L/R} = \mu$, and then, electrons from the occupied states $\varepsilon_d > \mu$ in the left hotter lead will tunnel through dot state ε_d to the empty state in the right colder lead, resulting in negative thermopopower $S < 0$. In **c**, $\varepsilon_d < \mu$, and then, the sign of the thermopower is reversed accordingly

$$H_{\mathrm{MBSs}} = i\delta_M \eta_1 \eta_2 + \lambda_1 (d_\uparrow - d_\uparrow^\dagger)\eta_1 + i\lambda_2 (d_\uparrow + d_\uparrow^\dagger)\eta_2, \quad (2)$$

in which δ_M is the overlap amplitude between the two MBSs with operator satisfying both $\eta_j = \eta_j^\dagger (j = 1, 2)$ and $\{\eta_i, \eta_j\} = \delta_{i,j}$. The hopping amplitude between MBSs and spin-↑ electrons in the QD is accounted by λ_j. It is helpful to write η_j in terms of the regular fermionic operators f as [18] $\eta_1 = (f^\dagger + f)/\sqrt{2}$ and $\eta_2 = i(f^\dagger - f)/\sqrt{2}$, and then, H_{MBSs} is rewritten as:

$$H_{\mathrm{MBSs}} = \delta_M \left(f^\dagger f - \frac{1}{2}\right) + \frac{\lambda_1}{\sqrt{2}} \left(d_\uparrow - d_\uparrow^\dagger\right)\left(f^\dagger + f\right) - \frac{\lambda_2}{\sqrt{2}} (d_\uparrow + d_\uparrow^\dagger)\left(f^\dagger - f\right). \quad (3)$$

We consider the system in linear response regime, i.e., under infinitely small bias voltage ΔV and temperature difference ΔT between the left and right leads, the electric and heat currents of each spin component are obtained as:

$$I_{e,\sigma} = -e^2 L_{0,\sigma} \Delta V + \frac{e}{T} L_{1,\sigma} \Delta T, \quad (4)$$

$$I_{h,\sigma} = e I_{1,\sigma} \Delta V - \frac{1}{T} L_{2,\sigma} \Delta T, \quad (5)$$

where e is the electron charge and T the system equilibrium temperature, and

$$L_{n,\sigma} = \frac{1}{\hbar} \int (\varepsilon - \mu)^n \left[-\frac{\partial f(\varepsilon, \mu)}{\partial \varepsilon}\right] T_\sigma(\varepsilon) \frac{d\varepsilon}{2\pi}, \quad (6)$$

where $\hbar$ is the reduced Planck's constant. We set the leads' chemical potential $\mu = 0$ as the energy zero point. The Fermi distribution function is given by $f(\varepsilon, \mu) = 1/\{1 + \exp[(\varepsilon - \mu)/k_B T]\}$ with k_B being the Boltzmann constant. The transmission coefficient $T_\sigma(\varepsilon)$ is calculated with the help of the retarded Green's function as:

$$T_\sigma(\varepsilon) = \frac{\Gamma_L \Gamma_R}{\Gamma_L + \Gamma_R} [-2\mathrm{Im} G_\sigma^r(\varepsilon)], \quad (7)$$

where $\Gamma_{L(R)} = 2\pi \sum_k |V_{kL(R)}|^2 \delta[\varepsilon - \varepsilon_{kL(R)}]$ is the linewidth function. We apply the standard equation of motion technique to obtain Green's function. The higher-order Green's functions are truncated by following scheme 2 in ref. [39], i.e., neglect the simultaneous tunneling of the electron of opposite spin. After some straightforward calculations, the spin-up retarded Green's function is given by:

$$G^r_{\uparrow}(\varepsilon) = \frac{\varepsilon_- - \Sigma_1^M - U\{1 - < n_\downarrow > [1 - (\lambda_1^2 - \lambda_2^2)^2 \tilde{B}\tilde{B}_U]\}}{(\varepsilon_- - \Sigma_0^M)(\varepsilon_- - U - \Sigma_1^M)}, \quad (8)$$

where the MBS-induced self-energies

$$\Sigma_0^M = B_1 + (\lambda_1^2 - \lambda_2^2)^2 B\tilde{B}, \quad (9)$$

and

$$\Sigma_1^M = B_1 + (\lambda_1^2 - \lambda_2^2)^2 B\tilde{B}_U, \quad (10)$$

with

$$B = \frac{\varepsilon}{\varepsilon^2 - \delta_M^2}, \quad (11)$$

$$B_1 = \frac{1}{2}\left(\frac{\lambda_1^2 - \lambda_2^2}{\varepsilon - \delta_M} + \frac{\lambda_1^2 + \lambda_2^2}{\varepsilon + \delta_M}\right), \quad (12)$$

$$\tilde{B} = \frac{B}{\varepsilon_+ + B_2}, \quad (13)$$

$$\tilde{B}_U = \frac{B}{\varepsilon_+ + U - B_2}, \quad (14)$$

in which

$$B_2 = \frac{1}{2}\left(\frac{\lambda_1^2 - \lambda_2^2}{\varepsilon + \delta_M} + \frac{\lambda_1^2 + \lambda_2^2}{\varepsilon - \delta_M}\right), \quad (15)$$

and $\varepsilon_\pm = \varepsilon \pm \varepsilon_d + i(\Gamma_L + \Gamma_R)/2$. In the absence of dot-MBSs hybridization ($\lambda_1 = \lambda_2 = 0$), we have $\Sigma_{0,1}^M = 0$ and $G^r_{\uparrow}(\varepsilon)$ recovers that of ref. [39]. It is also the spin-down retarded Green's function by changing $n_\downarrow$ into $n_\uparrow$. The occupation number is calculated self-consistently from:

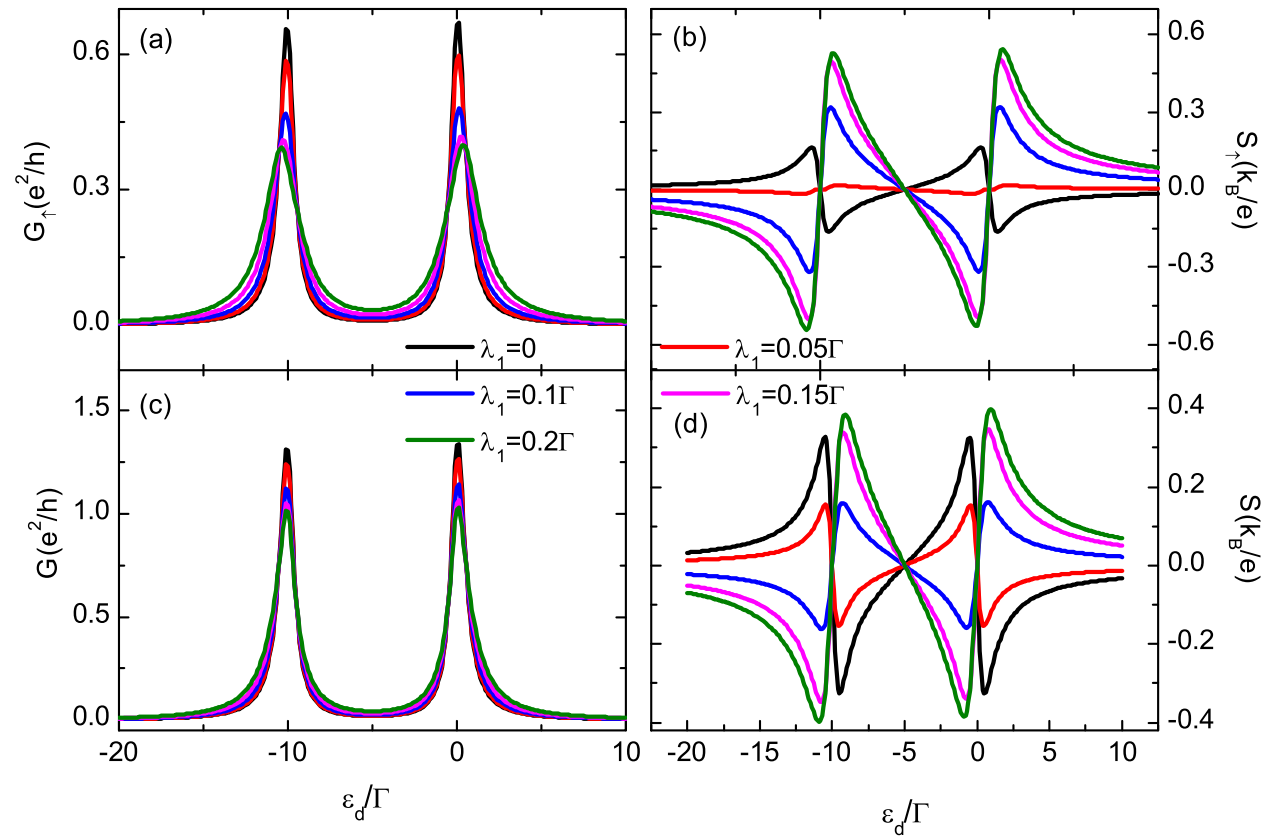

Fig. 2 Spin-dependent conductance and thermopower for different dot-Majorana coupling strengths (color online). The spin-up and total conductance in **a**, **c** and thermopower in **b**, **d** verse dot-level. The spin-down conductance and thermopower are almost unchanged by the dot-Majorana coupling strength λ_1, and they overlap with the black solid lines in **a** and **c**, respectively. Other parameters are temperature $T = 0.025\Gamma$, $\Delta_M = 0$, $U = 10\Gamma$, and $\lambda_2 = 0$

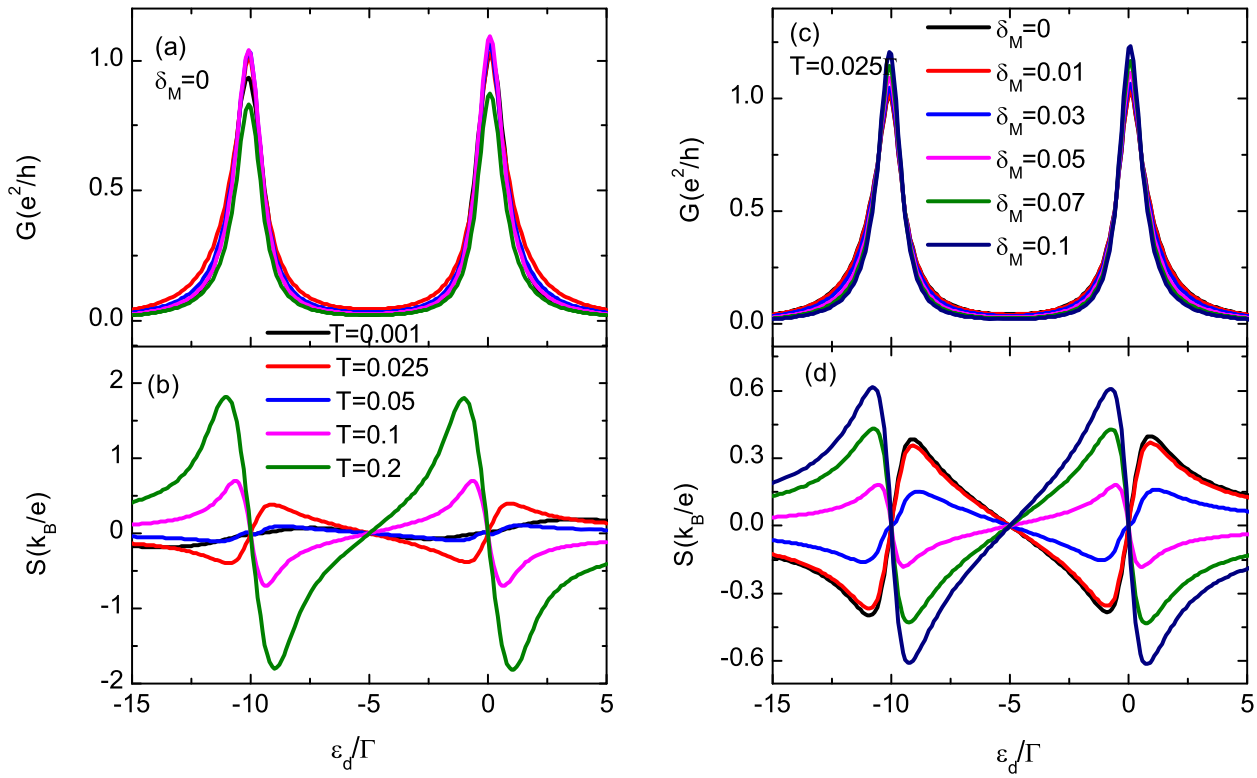

Fig. 3 Conductance and thermopower (color online). Counter plot of total conductance G and thermopower S as functions of ε_d and Δ_M in **a**, **b**, temperature T in **c**, **d**, respectively. The value of λ_1 is fixed as 0.2Γ. The temperature in **a**, **c** is 0.025Γ, and in **c**, **d** $\Delta_M = 0$. Other parameters are the same as those of Fig. 2

$$n_\sigma = \int \frac{d\varepsilon}{2\pi} \frac{\Gamma_L f_L(\varepsilon) + \Gamma_R f_R(\varepsilon)}{\Gamma_L + \Gamma_R} [-2\mathrm{Im} G^r_\sigma(\varepsilon)], \quad (16)$$

where $f_{L/R}(\varepsilon)$ is the Fermi distribution function in the left/right electrode.

Once the transmission function is obtained from Green's function, the electrical conductance and the thermopower (Seebeck coefficient) of each spin component are given by $G_\sigma = e^2 L_{0,\sigma}$ and $S_\sigma = -L_{1,\sigma}/(eTL_{0,\sigma})$, respectively.

Results and Discussions

In what follows, we assume symmetric coupling between the QD and electrodes, and set $\Gamma = 2\Gamma_L = 2\Gamma_R = 1$ as the energy unit. The intradot Coulomb interaction is fixed as $U = 10\Gamma$. We first study the case of the QD which is coupled to only MBS-1 with different hybridization strength λ_1 in Fig. 2 by setting $\lambda_2 = 0$. For $\lambda_1 = 0$, the conductance of each spin component in Fig. 2a develops two peaks located respectively at $\varepsilon_d = -\mu$ and $-\mu - U$. Note now the QD is free from spin polarization induced by the MBS, and the conductance of the two spin component is equal to each other ($G_\uparrow = G_\downarrow$), accordingly. Turning on the hybridization between the MBS and the QD ($\lambda_1 \neq 0$), the magnitude of $G_\uparrow$ is monotonously suppressed as shown in Fig. 2a, which is consistent with previous results [18, 34, 35]. The value of $G_\downarrow$, however, is almost unchanged even the occupation number $n_\downarrow$ is changed by λ_1 due to the presence of intradot Coulomb interaction (which is not shown in the figure). Meanwhile, the peaks' position and width in $G_\uparrow$ are slightly modified by the value of λ_1 due to the level renormalization by the dot-Majorana coupling [18, 34, 35]. The configuration of the total conductance $G = G_\uparrow + G_\downarrow$ in Fig. 2c resembles that of $G_\uparrow$.

The thermopower $S_\uparrow$ in Fig. 2b shows the typical sawtooth configuration and has three zero points individually at $\varepsilon_d = \mu$, $-U/2$, and $\mu - U$ [41, 42]. It develops a pair of sharp peaks with opposite signs at each of the two resonant states ($\varepsilon_d = \mu, \mu - U$) and changes sign whenever ε_d passes each zero points. In the absence of dot-MBSs hybridization ($\lambda_1 = 0$) as indicated by the solid black line in Fig. 2b, $S_\uparrow$ is positive (negative) when ε_d is below (above) the zero point as the main carriers are electrons (holes). With increasing λ_1, the spin-down thermopower $S_\downarrow$ is unchanged and the absolute value of $S_\uparrow$ firstly is suppressed and then enhanced. For sufficiently large λ_1, $S_\uparrow$ changes its sign as shown in Fig. 2b. With

further increased λ_1, the absolute value of $S_\uparrow$ exceeds that of $S_\downarrow$ and the total thermopower $S = S_\uparrow + S_\downarrow$ also changes its sign. Such a phenomenon has also been previously found in the spinless model [35–37]. In fact, the sign change of the thermopower in QD-based device without MBSs was attributed to several causes, such as the system equilibrium temperature [29], magnetic momentum of the electrodes [43], Coulomb interaction [43, 44], coupling strength between the QDs, the applied magnetic field, quantum interference effect, or the magnetic flux penetrating through multiple-dot ones [45, 46]. The above mechanisms are quite different from the present case, and the sign change of the thermopower by changing the hybridization between the QD and the MBSs is helpful for detecting the MBSs [35–37].

Figure 3a, b shows the total conductance G and thermopower S varying with the dot level ε_d for different values of the temperature T. The peak value of G is firstly enhanced and then suppressed by increasing temperature as shown in Fig. 3a. The magnitude of the thermopower in Fig. 3b, however, is mainly enhanced by increasing temperature, as there are more electrons (holes) excited above (below) the chemical potential. Moreover, S changes its sign for the cases of $T = 0.1$ and 0.2 as indicated by the pink and green lines in Fig. 3b, which is similar to the case of thermoelectric effect in QD-based structure without MBSs. For $T = 0.2\Gamma$, the peak value of S can reach as large as $2k_B/e$, which is one order of larger than that of $T = 0.001$. In fact, we have checked that the magnitude of the thermopower can be further enhanced by increasing the temperature. In the present paper, however, we focus on the sign change of S at relatively low temperature, which is usually the case of the MBSs formed in experiments. Figure 3c, d presents the conductance and the thermopower for different values of direct hybridization of the two MBSs at opposite ends of the nanowire at fixed $T = 0.025\Gamma$. The peak value of the conductance in Fig. 3c is monotonously enhanced by increasing δ_M, which is in consistent with the results found by López et al. [35]. The thermopower in Fig. 3d changes its sign for $0.03\Gamma < \delta_M < 0.05\Gamma$, which is larger than the temperature $T = 0.025\Gamma$. In ref. [32], they found that the thermopower changes its sign at about $\delta_M \approx k_B T$ in the spinless model. In the present paper, the sign change of S occurs at relatively larger δ_M as the MBSs are coupled to only one spin direction electrons. Moreover, the peak value of the thermopower can also be enhanced by increasing δ_M.

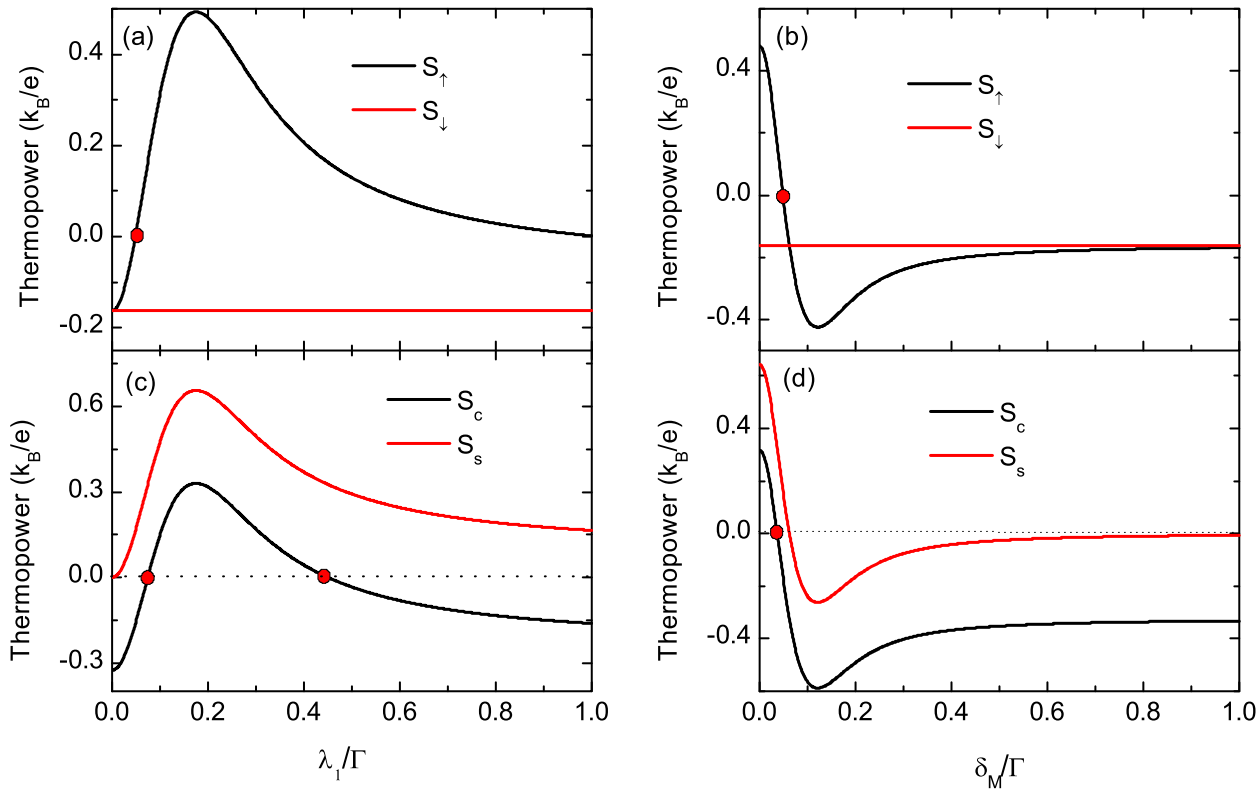

Fig. 4 Thermopowers varying with dot-Majorana coupling strength and direct overlap. The thermopowers as functions of λ_1 in **a**, **b** with $\Delta_M = 0$, and Δ_M in **c**, **d** with $\lambda_1 = 0.2\Gamma$, respectively. Other parameters are the same as those of Fig. 2

We show the spin-resolved thermopowers individually as functions of λ_1 and δ_M in Fig. 4. The spin-up thermopower $S_\uparrow$ in Fig. 4a firstly increases, reaching a maximum and then decreases with increasing λ_1. At sufficiently large λ_1, it remains at a stable value. The value of spin-down thermopower $S_\downarrow$ is unchanged by λ_1 as expected. The behaviors of $S_\uparrow$ and $S_\downarrow$ bring about two interesting results: one is the 100% spin-polarized thermopower when $S_\uparrow = 0$ but $S_\downarrow$ has a finite value that can be used for filtering electron spin; the other is the finite pure spin thermopower $S_s = S_\uparrow - S_\downarrow$ with zero charge thermopower $S_c = S_\uparrow + S_\downarrow = 0$ which occurred when $S_\uparrow = -S_\downarrow$ as shown by the dots in Fig. 4b. At closed circuit, the 100% spin-polarized and pure spin thermopowers are individually the corresponding currents, which are virtual in spintronic devices. Similar results are found in Fig. 4b, d, in which $S_\uparrow$ undergoes sign change by changing δ_M, whereas $S_\downarrow$ keeps unchanged. We emphasize that the present 100% spin-polarized and pure spin thermopowers emerge in the absence of magnetic field or magnetic materials in the QD.

In Fig. 5, we study the case of both the MBSs at the opposite ends of the nanowire which are coupled to the QD when the wire and the dot are close to each other enough with $\delta_M = 0$. Figure 5a shows that the total conductance G keeps the double-peak configuration in the presence of λ_2. The peaks' height will be suppressed by increasing λ_2. The lineshape of S is also unchanged by the value of λ_2 as indicated by Fig. 5b. The peak's value of S will be significantly enhanced since the thermopower is reversely proportional to the conductance. For $\lambda_2 \sim 0.2\Gamma$, the magnitude of the thermopower can reach as large as $2k_B/e$. Moreover, we find that S will not change its sign by adjusting the value of λ_2. Figure 6 shows the total thermopower as a function of ε_d for different values of direct hybridization between the MBSs δ_M by fixing $\lambda_1 = \lambda_2 = 0.2\Gamma$. It shows that both the magnitude and the sign can be effectively changed by tuning δ_M, which is similar to the case that only one of the MBSs is coupled to the QD. Finally, we briefly discuss the experimental realization of the present devices. The nanowire hosting the MBSs can be fabricated with InAs grown by molecular beam epitaxy with several nanometers of epitaxial Al layer [47]. It has been experimentally proven that a hard superconducting gap can be induced on such a kind of nanowires [47, 48] by applying a critical magnetic field exceeding 2 T along the wire axis [20]. A QD is formed in the bare InAs segment at the end of the wire due to density of state gradients at the edges of the Al shell [20, 47, 48].

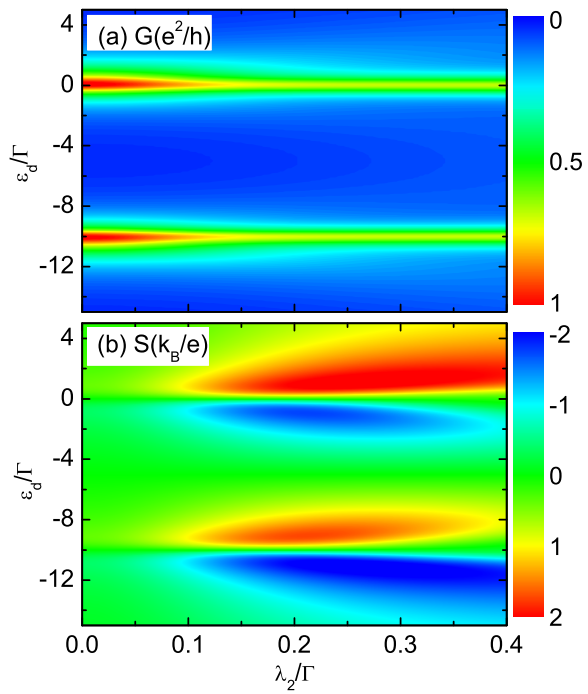

Fig. 5 Impacts of the other dot-Majorana coupling on the thermopower (color online). Impacts of λ_2 on the total conductance (**a**) and thermopower (**b**) with $\lambda_1 = 0.2\Gamma$, $\delta_M = 0$. Other parameters are the same as those of Fig. 2

Conclusions

In conclusion, we have studied the properties of the electrical conductance and thermopower in a quantum dot connected to the left and right normal metal electrodes with Coulomb interaction. The dot is also coupled to MBSs formed in a semiconducting nanowire. We find that the MBSs influence the conductance and

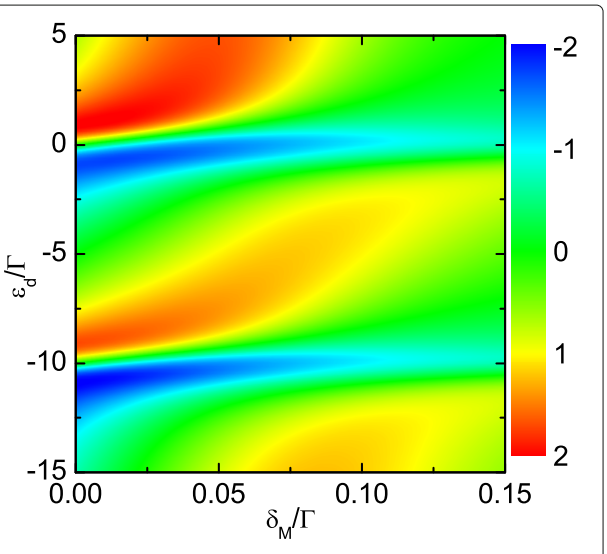

Fig. 6 Counter plot of the thermopower (color online). Counter plot of the thermopower as a function of ε_d and λ_2 for $\lambda_1 = 0.2\Gamma$. Other parameters are the same as those of Fig. 2

thermopower of the spin component it only couples to, although the spin-up and spin-down electrons interact to each other via the Coulomb repulsion. The sign of the thermopower can be changed by adjusting the dot-MBSs hybridization strength, the direction hybridization between the MBSs, and the system temperature. Large value of either 100% spin-polarized or pure spin themropowers can be obtained in non-magnetic QD structure. The coupling between the dot and both the two MBSs can only change the magnitude of the thermopower, but not its sign. Our results may be useful in detecting the existence of the MBSs via thermoelectric technique.

Abbreviations

QD: Quantum dot; MBSs: Majorana bound states

Acknowledgments

This work was supported by the National Natural Science Foundation of China (grant no. 11675023). Fu acknowledges the Innovation Development Fund of China Academy of Engineering Physics (CAEP) (grant no. ZYCX1921-02) and the Presidential Foundation of CAEP (grant no. YZ2015014). Liu acknowledges the NSF of InnerMongolia (grant no.2017MS0112), and Science Foundation for excellent Youth Scholars of Inner Mongolia University of science and technology (grant no. 2017YQL06). Chi is supported by the Initial Project of UEST of China, Zhongshan Institute (415YKQ02), Science and Technology Bureau of Zhongshan (grant nos. 2017B1116, 2017B1016). This work is also supported by the Innovation Team of Zhongshan City (no. 170615151170710).

Authors' Contributions

Fu Z.G. and Chi F. contributed the ideas and derived the formulae in the paper. Chi F., Li K.M, and Liu J. performed the numerical calculations. Chi F. and Fu Z.G. wrote the original manuscript. All authors revised the paper. The authors read and approved the final manuscript.

Availability of Data and Materials

The datasets supporting the conclusions of this article are included within the article.

Competing Interests

The authors declare that they have no competing interests.

Author Details

[1]School of Electronic and Information Engineering, University of Electronic Science and Technology of China, Zhongshan Institute, Shiqi District Xueyuan Road No. 1, Zhongshan, 528402, China. [2]Institute of Applied Physics and Computational Mathematics, No. 6 Huayuan Road, Haidian District, Beijing, 100088, China. [3]School of Science, Inner Mongolia University of Science and Technology, Kundu District Alding Road No. 7, Baotou, 014010, China.

Received: 26 August 2019 Accepted: 24 March 2020
Published online: 15 April 2020

References

1. C. Nayak, S. H. Simon, A. Stern, M. Freedman, S. D. Sarma, Non-Abelian anyons and topological quantum computation. Rev. Mod. Phys. **80**, 1083 (2008)
2. J. Alicea, Y. Oreg, G. Refael, F. Oppen, M. P. A. Fisher, Non-Abelian statistics and topological quantum information processing in 1D wire networks. Nat. Phys. **7**, 412 (2011)
3. T. Karzig, C. Knapp, R. M. Lutchyn, P. Bonderson, M. B. Hastings, C. Nayak, J. Alicea, K. Flensberg, S. Plugge, Y. Oreg, C. M. Marcus, M. H. Freedman, Scalable designs for quasiparticle-poisoning-protected topological quantum computation with Majorana zero modes. Phys. Rev. B. **95**, 235305 (2017)
4. X. Liu, X. Li, D. L. Deng, X. J. Liu, S. D. Das, Majorna spintronics. Phys. Rev. B. **94**, 014511 (2016)
5. M. Sato, S. Fujimoto, Topological phases of noncentrosymmetric superconductors: edge states, Majorana fermions, and non-Abelian statistics. Phys. Rev. B. **79**, 094504 (2009)
6. X. L. Qi, S. C. Zhang, Topological insulators and superconductors. Rev. Mod. Phys. **83**, 1057 (2011)
7. M. Wimmer, A. R. Akhmerov, M. V. Medvedyeva, J. Tworzydło, C. W. J. Beenakker, Majorana bound states without vortices in topological superconductors with electrostatic defects. Phys. Rev. Lett. **105**, 046803 (2010)
8. J. D. Sau, R. M. Lutchyn, S. Tewari, S. D. Sarma, Generic new platform for topological quantum computation using semiconductor heterostructures. Phys. Rev. Lett. **104**, 040502 (2010)
9. R. M. Lutchyn, J. D. Sau, S. D. Sarma, Majorana fermions and a topological phase transition in semiconductor-superconductor heterostructures. Phys. Rev. Lett. **105**, 077001 (2010)
10. T. P. Choy, J. M. Edge, A. R. Akhmerov, C. W. J. Beenakker, Majorana fermions emerging from magnetic nanoparticles on a superconductor without spin-orbit coupling. Phys. Rev. B. **84**, 195442 (2011)
11. P. San-Jose, E. Prada, R. Aguado, AC Josephson effect in finite-length nanowire junctions with Majorana modes. Phys. Rev. Lett. **108**, 257001 (2011)
12. D. Laroche, D. Bouman, D. J. van Woerkom, A. Proutski, C. Murthy, D. I. Pikulin, C. Nayak, R. J. J. van Gulik, J. Nygård, P. Krogstrup, L. P. Kouwenhoven, A. Geresdi, Observation of the 4π-periodic Josephson effect in indium arsenide nanowires. Nat. Commun. **10**, 245 (2019)
13. Q. L. He, L. Pan, A. L. Stern, E. C. Burks, X. Che, G. Yin, J. Wang, B. Lian, Q. Zhou, E. S. Choi, K. Murata, X. Kou, Z. Chen, T. Nie, Q. Shao, Y. Fan, S. C. Zhang, K. Liu, J. Xia, K. L. Wang, Chiral Majorana fermion modes in a quantum anomalous Hall insulator-superconductor structure. Science. **357**, 294 (2017)
14. V. Mourik, K. Zuo, S. M. Frolov, S. R. Plissard, E. P. A. M. Bakkers, L. P. Kouwenhoven, Signatures of Majorana fermions in hybrid superconductor-semiconductor nanowire devices. Science. **336**, 1003 (2012)
15. S. Nadj-Perge, I. K. Drozdov, J. Li, H. Chen, S. Jeon, J. Seo, A. H. MacDonald, B. B. Andrei, A. Yazdani, Observation of Majorana fermions in ferromagnetic atomic chains on a superconductor. Science. **346**, 602 (2014)
16. W.iel. van der W.G., S. D. Franceschi, J. M. Elzerman, T. Fujisawa, S. Tarucha, L. P. Kouwenhoven, Electron transport through double quantum dots. Rev. Mod. Phys. **75**, 1 (2003)
17. Z. M. Wang, *Self-assembled quantum dots*. (Springer, New York, 2008)
18. D. E. Liu, H. U. Baranger, Detecting a Majorana-fermion zero mode using a quantum dot. Phys. Rev. B. **84**, 201308(R) (2011)
19. E. Vernek, P. H. Penteado, A. C. Seridonio, J. C. Egues, Thermopower of three-terminal topological superconducting systems. Phys. Rev. B. **89**, 165314 (2014)
20. M. T. Deng, S. Vaitiekenas, E. B. Hansen, J. Danon, M. Leijnse, K. Flensberg, J. Nygård, P. Krogstrup, C. M. Marcus, Majorana bound state in a coupled quantum-dot hybrid-nanowire system. Science. **354**, 1557 (2016)
21. H. J. Chen, K. D. Zhu, Nonlinear optomechanical detection for Majorana fermions via a hybrid nanomechanical system. Nanoscale Res. Lett. **9**, 166 (2014)
22. H. J. Chen, K. D. Zhu, All-optical scheme for detecting the possible Majorana signature based on QD and nanomechanical resonator systems. Sci. China Phys. Mech. Astron. **58**, 050301 (2015)
23. Y. X. Li, Z. M. Bai, Tunneling transport through multi-quantum-dot with Majorana bound states. J. Appl. Phys. **114**, 033703 (2013)
24. N. Wang, S. H. Lv, Y. X. Li, Quantum transport through the system of parallel quantum dots with Majorana bound states. J. Appl. Phys. **115**, 083706 (2014)
25. W. J. Gong, S. F. Zhang, Z. C. Li, G. Y. Yi, Y. S. Zheng, Detection of a Majorana fermion zero mode by a T-shaped quantum-dot structure. Phys. Rev. B. **89**, 245413 (2014)
26. A. Ueda, T. Yokoyama, Anomalous interference in Aharonov-Bohm rings with two Majorana bound states. Phys. Rev. B. **90**, 081405(R) (2014)
27. J. J. Xia, S. Q. Duan, W. Zhang, Detection of Majorana fermions by Fano resonance in hybrid nanostructures. Nanoscale Res. Lett. **10**, 223 (2015)
28. C. Jiang, Y. S. Zheng, Fano effect in the Andreev reflection of the Aharonov-Bohm-Fano ring with Majorana bound states. Solid State Commun. **212**, 14 (2015)

29. Y. Dubi, M. D. Ventra, Colloquium: heat flow and thermoelectricity in atomic and molecular junctions. Rev. Mod. Phys. **83**, 131 (2013)
30. B. Sothmann, R. Sánchez, A. N. Jordan, Thermoelectric energy harvesting with quantum dots. Nanotechnology. **26**, 032001 (2015)
31. H. Thierschmann, R. Sánchez, B. Sothmann, F. Arnold, C. Heyn, W. Hansen, H. Buhmann, L. W. Molenkamp, Three-terminal energy harvester with coupled quantum dots. Nat. Nanotechnol. **10**, 854 (2016)
32. A. Marcos-Vicioso, C. López-Jurado, M. Ruiz-Garcia, R. Sánchez, Thermal rectification with interacting electronic channels: exploiting degeneracy, quantum superpositions, and interference. Phys. Rev. B. **98**, 035414 (2018)
33. C. Y. Hou, K. Shtengel, G. Refael, Thermopower and Mott formula for a Majorana edge state. Phys. Rev. B. **88**, 075304 (2013)
34. M. Leijinse, Thermoelectric signatures of a Majorana bound state coupled to a quantum dot. New. J. Phys. **16**, 015029 (2014)
35. R. López, M. Lee, L. Serra, J. S. Lim, Thermoelectrical detection of Majorana states. Phys. Rev. B. **89**, 205418 (2014)
36. L. S. Ricco, F. A. Dessotti, I. A. Shelykh, M. S. Figueira, A. C. Seridonio, Tuning of heat and charge transport by Majorana fermions. Scient. Rep. **8**, 2790 (2018)
37. S. Valentini, R. Fazio, V. Giovannetti, F. Taddei, Thermopower of three-terminal topological superconducting systems. Phys. Rev. B. **91**, 045430 (2015)
38. N. V. Gnezdilov, M. Diez, M. J. Pacholski, C. W. J. Beenakker, Wiedemann-Franz-type relation between shot noise and thermal conduction of Majorana surface states in a three-dimensional topological superconductor. Phys. Rev. B. **94**, 115415 (2016)
39. S. Smirnov, Universal Majorana thermoelectric noise. Phys. Rev. B. **97**, 165434 (2018)
40. J. Barański, A. Kobiałka, T. Domanski, Spin-sensitive interference due to Majorana state on the interface between normal and superconducting leads. J. Phys. Condens. Matter. **29**, 075603 (2017)
41. J. Liu, Q. F. Sun, X. C. Xie, Enhancement of the thermoelectric figure of merit in a quantum dot due to the Coulomb blockade effect. Phys. Rev. B. **81**, 245323 (2010)
42. F. Chi, J. Zheng, X. D. Lu, K. C. Zhang, Thermoelectric effect in a serial two-quantum-dot. Phys Lett A. **375**, 1352 (2011)
43. W. P. Xu, Y. Y. Zhang, Q. Wang, Z. J. Li, Y. H. Nie, Thermoelectric effects in triple quantum dots coupled to a normal and a superconducting leads. Phys. Lett. A. **380**, 958 (2016)
44. G. Rajput, P. K. Ahluwalia, K. C. Sharma, Thermoelectric properties of correlated double quantum dot system in Coulomb blockade regime. Physica B. **406**, 3328 (2011)
45. Y. M. Blanter, C. Bruder, R. Fazio, H. Schoeller, Aharonov-Bohm-type oscillations of thermopower in a quantum-dot ring geometry. Phys. Rev. B. **55**, 4069 (1997)
46. Y. S. Liu, F. Chi, X. F. Yang, J. F. Feng, Pure spin thermoelectric generator based on a Rashba quantum dot molecule. J. Appl. Phys. **109**, 053712 (2011)
47. M. T. Deng, S. Vaitiek enas, E. Prada, P. San-Jose, J. Nygard, P. Krogstrup, R. Aguado, C. M. Marcus, Nonlocality of Majorana modes in hybrid nanowires. Phys. Rev. B. **98**, 085125 (2018)
48. W. Chang, S. W. Albrecht, T. S. Jespersen, F. Kuemmeth, P. Krogstrup, J. Nygôd, C. M. Marcus, Hard gap in epitaxial semiconductor-superconductor nanowires. Nat. Nanotechnol. **10**, 232 (2015)

Publisher's Note